

# DuoMorph: Synergistic Integration of FDM Printing and Pneumatic Actuation for Shape-Changing Interfaces

Xueqing Li  
li-xq23@mails.tsinghua.edu.cn  
Tsinghua University / The Hong Kong  
Polytechnic University  
Beijing / Hong Kong, China

Danqi Huang  
hdq24@mails.tsinghua.edu.cn  
Tsinghua University  
Beijing, China

Tianyu Yu  
tianyuyu@berkeley.edu  
University of California, Berkeley  
Berkeley, CA, USA

Shuzi Yin  
yinsz24@mails.tsinghua.edu.cn  
Tsinghua University  
Beijing, China

Bingjie Gao  
gbj24@mails.tsinghua.edu.cn  
Tsinghua University  
Beijing, China

Anna Matsumoto  
antech33@stanford.edu  
Stanford University  
Stanford, CA, USA

Zhihao Yao  
yaozh\_h@outlook.com  
Tsinghua University  
Beijing, China

Yiwei Zhao  
18009238328@163.com  
Tsinghua University  
Beijing, China

Shiqing Lyu  
lvsq22@mails.tsinghua.edu.cn  
Tsinghua University  
Beijing, China

Yuchen Tian  
1849859198@qq.com  
Tsinghua University  
Beijing, China

Lining Yao  
liningy@berkeley.edu  
University of California, Berkeley  
Berkeley, CA, USA

Haipeng Mi  
haipeng.mi@gmail.com  
Tsinghua University  
Beijing, China

Qiuyu Lu\*  
qiuyu.lu@polyu.edu.hk  
Interbeing Lab, School of Design  
The Hong Kong Polytechnic  
University  
Hong Kong, China



**Figure 1: DuoMorph overview.** (a) Design tool for modeling and generating integrated G-code; (b) Fabrication of heat-sealed pneumatic actuators (left) and subsequent printing of structures directly on top (right) using an FDM printer; (c) Preshaping the pneumatic actuator with 4D-printed structures in hot water; (d, e) A mimosa-inspired interactive sculpture that folds when touched and blooms when left alone. The flower is also fabricated through a same process.

\*Corresponding author



This work is licensed under a Creative Commons Attribution 4.0 International License.  
CHI '26, Barcelona, Spain

© 2026 Copyright held by the owner/author(s).  
ACM ISBN 979-8-4007-2278-3/2026/04  
<https://doi.org/10.1145/3772318.3791040>

## Abstract

We introduce DuoMorph, a design and fabrication method that synergistically integrates Fused Deposition Modeling(FDM) printing and pneumatic actuation to create novel shape-changing interfaces. In DuoMorph, the printed structures and heat-sealed pneumatic elements are mutually designed to actuate and constrain each other, enabling functions that are difficult for either component to achieve in isolation. Moreover, the entire hybrid structure can be fabricated through a single, seamless process using only a standard FDM

printer—including both heat-sealing and 3D/4D printing. In this paper, we define a design space including four primitive categories that capture the fundamental ways in which printed and pneumatic components can interact. To support this process, we present a fabrication method and an accompanying design tool. Finally, we demonstrate the potential of DuoMorph through example applications and performance demonstrations.

## CCS Concepts

• **Human-centered computing** → **Interactive systems and tools.**

## Keywords

Shape-Changing Interface; Fabrication; Pneumatic Interface; FDM Printing; 4D Printing

### ACM Reference Format:

Xueqing Li, Danqi Huang, Tianyu Yu, Shuzi Yin, Bingjie Gao, Anna Matsumoto, Zhihao Yao, Yiwei Zhao, Shiqing Lyu, Yuchen Tian, Lining Yao, Haipeng Mi, and Qiuyu Lu. 2026. DuoMorph: Synergistic Integration of FDM Printing and Pneumatic Actuation for Shape-Changing Interfaces. In *Proceedings of the 2026 CHI Conference on Human Factors in Computing Systems (CHI '26)*, April 13–17, 2026, Barcelona, Spain. ACM, New York, NY, USA, 14 pages. <https://doi.org/10.1145/3772318.3791040>

## 1 Introduction

Pneumatic interfaces have gained significant traction in Human-Computer Interaction (HCI) and soft robotics due to their lightweight, compliance, and reversible actuation [27, 47, 48]. They have enabled a wide range of applications, from shape-changing displays [10, 15, 48, 50] and haptic feedback [5, 7, 11] to multifunctional robotic systems [16–18]. However, fabricating soft pneumatic actuators remains challenging. Casting approaches support complex geometries but require molds and labor-intensive processes [22, 48]. 3D printing provides digital fabrication capabilities, yet reversible pneumatic actuators often rely on costly elastic-resin-based processes such as SLA (Stereolithography) [38], while FDM-printed actuators are typically irreversible due to material constraints [42]. In the meanwhile, heat sealing offers a low-cost and accessible alternative that can produce diverse actuation behaviors with simple tools, and is often adopted in making shape-changing interfaces [15, 25, 27, 45].

Recent efforts have adapted consumer-grade FDM printers for heat sealing, lowering barriers to entry [4, 47]. However, these works largely stop at heat sealing alone, without exploring the integration of heat sealing with FDM printing. This raises several design curiosities: What happens if we continuously print on sealed air bags? How should the structural design and fabrication process be tuned? How reliably can printed structures bond with the airbags? And most importantly, what new capabilities emerge when the two are combined?

Motivated by these curiosities, we developed DuoMorph, a design and fabrication method that synergistically integrates FDM printing and pneumatic actuation to create novel shape-changing interfaces (Fig. 1). In DuoMorph, printed structures and pneumatic elements are designed to actuate and constrain each other, enabling

functions that neither could hardly achieve alone. Moreover, the entire hybrid structure can be fabricated in a single, seamless process using only a standard FDM printer—including both heat sealing and 3D/4D printing. This approach enables a streamlined, more precise, and more consistent process, while significantly reducing labor compared to preparing pneumatic actuators and printed parts separately and then manually gluing and assembling them.

Based on this principle, we define a design space comprising four primitive categories that capture the fundamental ways in which pneumatic and printed components can interact. To support this process, we present an integrated fabrication method and a design tool that automatically generates G-code for production. Finally, we demonstrate DuoMorph's potential through a series of application examples and performance evaluations.

The contributions of this work are threefold:

- A synergistic design strategy that leverages the interaction between pneumatic actuators and FDM printed structures to enable functions that either component alone can hardly achieve.
- An integrated fabrication workflow and accompanying design tool that unify heat sealing and FDM printing into a single streamlined process.
- Application demonstrations and evaluations that showcase the expressive and functional capabilities of DuoMorph in interactive systems.

## 2 Related Works

**Pneumatic Interfaces.** Pneumatic interfaces, emerging from the field of soft robotics, have been widely studied in HCI [8, 19, 20, 36], due to their potential to safely bridge the gap between machines and people, a capability rooted in their inherent compliance and adaptability [30]. Inflatable structures particularly offer several advantages for interaction design, including being lightweight, cost-effective, scalable, and easily stored [2, 47]. However, the fabrication and control of these interfaces have been central research challenges that have evolved over time [30].

Fabrication of early pneumatic actuators often involved techniques such as molding and casting of silicone rubbers, which required intensive manual labor and limited design flexibility for complex geometries [30, 43]. Meanwhile, researchers explored a more accessible and rapid approach using heat-sealed thermoplastic films with embedded programmable folds, which allows the fabrication of inflatable geometries [27, 31, 47, 48]. This approach was extended with multilayer techniques that produce more complex 3D deformations and functionalities [16, 51], and was further developed by repurposing standard FDM 3D printers as heat-sealing tools [4, 28].

While much of the research focused on the geometry of the seal itself, some research has also explored how to enhance the capability of these pneumatic structures by integrating external or additional components. One approach involved the addition of non-inflatable materials to control deformation. For example, PneuUI added multilayer structures with different mechanical or electrical properties, such as paper or conductive thread [48], while BlowFab engraved patterns with a resistant resin or heat-resistant film onto plastic sheets to control the bending and texture of the final

shape [44]. Others have added separate mechanical components to enable more complex behaviors, such as passive check valves for sequential control [3]. Furthermore, fluidic logic systems enabled electronics-free control through custom valves and circuits [3, 6, 17]. Specific approaches include miniaturizing fluidic chambers for high-resolution, sequential control [15], and more recently, designing pneumatic "coding blocks" that function like software 'If' or 'For' statements, enabling autonomous, decision-making behaviors [29].

To support creativity and rapid prototyping, previous research, including Pneuduino, pioneered in modular hardware toolkits to manage complex systems for pneumatic interfaces [12, 14, 26], and further research was done to make them compact and more comprehensive [23, 33, 37]. PneuBots [49] introduced a construction kit with various inflatable modules and pneumatic connectors and splitters, allowing users to assemble diverse structures.

**FDM/SLA Printed Interactive Devices.** Separate from inflatables, FDM printing has been widely explored as a low-cost and accessible approach for fabricating interactive devices. A significant research direction explores 4D printing, where printed objects are programmed to transform over time in response to external stimuli [21]. FDM has been essential in this domain for creating heat-activated composites, enabling complex deformations such as the self-folding from 2D to 3D [1], the programmable bending of linear structures [40], and the morphing of mesh surfaces [41]. Beyond shape transformation, the FDM process offers fine control, as seen in quasi-woven textiles [9], 3D weaving [34], tunable hair-like structures [39], and expressive textures created by manipulating extruder parameters [35].

More recently, research has been focused on embedding pneumatic functions directly into FDM-printed artifacts. This includes systems that integrate electronics-free pneumatic logic gates and I/O directly into a 3D model's geometry [32] and toolkits that provide libraries of printable pneumatic widgets for rapid prototyping [13]. While these systems successfully embed pneumatic logic or actuation, they remain distinct from methods that create inflatable structures from soft films, requiring the combination of the FDM print with a separate process like blow molding [42]. Beyond FDM, Stereolithography (SLA) has also been utilized to create fluid-driven devices [46].

**Combination of FDM/SLA printing and Pneumatic Actuation.** A smaller body of work has sought to combine 3D-printing and pneumatic actuation explicitly. Stereolithography (SLA) has been used to fabricate reversible pneumatic actuators directly, though these methods often rely on specialized and costly elastic resins [46]. FDM-based approaches, in contrast, while offering the potential for multi-material printing, have still typically produced actuators that are either part of a multi-step, hybrid workflow—such as creating pre-forms for blow molding—or whose shape changes are irreversible due to material constraints [42]. Other methods repurpose the printer as a single-function tool, using its heated nozzle solely to heat-seal separate thermoplastic films [4, 47] or a speed-modulated ironing tool [28]. Therefore, the challenge of a single, unified, low-cost workflow that uses a standard FDM printer to seamlessly fabricate 3D structural components and create reversible, heat-sealed inflatables remains largely unexplored. To address this gap, we introduce a novel methodology that seamlessly integrates FDM printing and heat-sealing in a single, accessible process.

### 3 Design Space

Based on how the printed structures interact with the pneumatic actuators, we propose a four-dimensional design space, categorized according to the functions served by the printed structures as shown in Fig. 2:

- Passive Deformation Structures, which respond to deformation of the pneumatic actuator;
- Constraining Structures, which regulate deformation of the pneumatic actuator;
- Pre-shaping Structures, which impose a preset geometry before actuation;
- Function-Extending Structures, which extend the capabilities of the device beyond deformation

This section will explain these dimensions with example primitives.

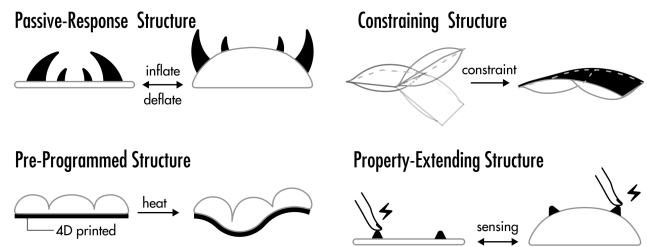


**Figure 2: The four-dimensional design space of DuoMorph, categorized based on how the printed structures (black) would interact with the pneumatic actuators (gray) .**

#### 3.1 Passive Deformation Structure

The printed structure can locomote or deform as the pneumatic actuator inflates or deflates. For example, Fig. 3.a shows the printed petals blooming simultaneously when the airbag is inflated. If the structures are distributed across different chambers, they can also be actuated asynchronously (Fig. 3.b). Moreover, a single structure may span multiple chambers; in this case, it can move in different directions depending on which chamber is inflated (Fig. 3.c).

#### 3.2 Constraining Structure

The printed structures can also influence how pneumatic actuators deform when inflated, serving as constraints. First, they can be used to reconfigure the bending angle of an airbag, which is conventionally tuned through sealing patterns and becomes fixed once sealed. As shown in Fig. 4.a, a triangular slider along a rail can stop the airbag at different angles, offering tunability. Second, continuous printed layers on the airbag surface can reinforce specific regions, thereby controlling the actuator's bending direction (Fig. 4.b). Finally, connectors can be directly printed onto the airbag, enabling easy assembly of multiple airbags into various configurations (Fig. 4.c).

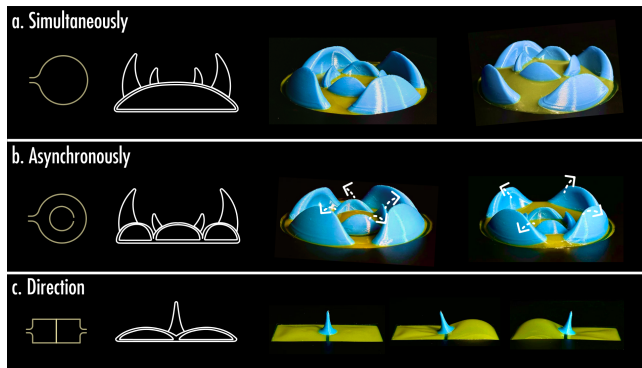


Figure 3: Example printed passive structure. The structures are actuated (a) simultaneously, (b) asynchronously, and (c) toward different directions by the airbags.

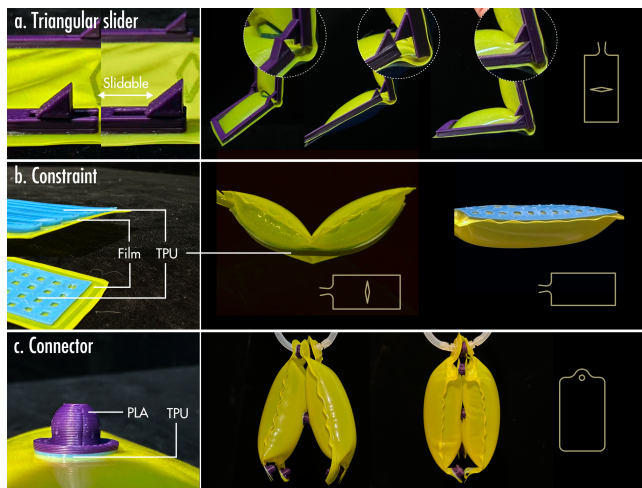


Figure 4: Example printed constraint structures that can control how the airbags deform when inflated include: (a) structures that allow tuning of the bending angle, (b) patterns that change or reverse the bending direction, and (c) connectors that enable assembling multiple airbags into more complex configurations.

### 3.3 Pre-shaping Structure

The pre-shaping deformation structure can deform the pneumatic actuator into desired shapes using 4D printing techniques. Although pneumatic actuators can achieve 3D deformation independently, integrating 4D-printed structures offloads part of this responsibility, simplifies actuator design, and frees internal chambers to focus on other functions (e.g., enhancing the movement of passive-deformation structures).

Fig 5 shows some example designs. In Fig. 5.a, the actuator made from a TPU film effectively serves as—and replaces—the TPU layer in conventional 4D printed structures. When heated, the printed PLA layer contracts while the TPU film remains stable, forcing the pneumatic actuator to bend upward to the side with the printed structures (concave bending). The achievement of bending in the

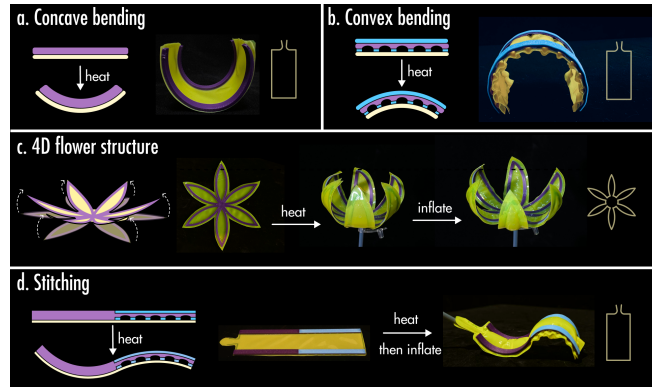


Figure 5: Example 4D printed pre-shaping structures that can preshape the airbags. When heated, the primitives (a) Bend toward the printed structure side (concave bending); (b) Bend toward the other side (convex bending); (c,d) Deform to complex shapes.

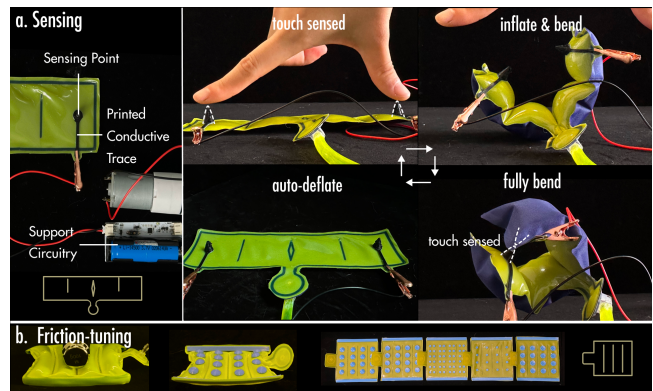


Figure 6: Example printed enabling structures that extend the capabilities of pneumatic actuators beyond deformation: (a) adding sensing capability, (b) tuning surface friction.

opposite direction (convex bending) is less straightforward. In conventional 4D printing, this can be done by simply switching the TPU layer from the bottom to the top. However, in the DuoMorph fabrication process, the TPU film can serve only as the bottom layer. To address this limitation, we propose the structure shown in Fig. 5.b: here, the bottom continuous-arched pattern enables PLA to adhere to the TPU film discontinuously, allowing this side to contract upon heating. Meanwhile, the top side has a printed TPU layer that constrains PLA shrinkage, causing the actuator to bend downward. By combining these basic deformation modes, more complex shape changes can be achieved (Fig. 5.c, d).

### 3.4 Function-Extending Structure

The printed structures can be leveraged to extend the capabilities of pneumatic actuators beyond deformation, enabling new functions. For example, by using conductive filament, structural features and

circuit traces can be directly printed onto the airbag to add sensing capabilities. As shown in Fig. 6.a, one primitive demonstrates an airbag that inflates to bend when touched, then automatically deflates and returns after fully bending. Another direction we explored is tuning the surface friction of the airbag. Fig. 6.b illustrates a series of primitives with dot arrays of varying sizes and densities. Experiments show that different patterns produce distinct levels of friction adjustment (section.6.3)

## 4 Fabrication

### 4.1 Walkthrough

Our overall workflow is illustrated in Fig. 7, achieving **integrated fabrication of heat sealing and printing** through FDM printers. In the design phase, we developed and integrated multiple parametric tools (such as heat sealing and 4D printing) in the Rhino and Grasshopper environment, and built a user interface based on HumanUI to support integrated operations and improve production efficiency. During fabrication, we used a standard single-nozzle Bambu Lab A1 Series 3D printer for integrated heat sealing and printing. If multiple filament types are required, manual filament swapping or Bambu Lab’s AMS (Automatic Material System) can be used. The musical prompt function acts as an audio reminder for the next step so the user doesn’t have to keep an eye on the printer.

### 4.2 Digital Design

To help users understand the DuoMorph workflow and simplify design and fabrication operations, we developed a GUI design tool based on the Rhino 8 computer-aided design (CAD) tool and the built-in Grasshopper plugin, shown in Fig. 8.a. This tool supports users in converting custom planar sketches into G-code for heat sealing airbags using 3D printers, and merging them with G-code for other components requiring 3D printing to obtain the final complete fabrication G-code.

The specific usage process is as follows:

- (1) **Define the printing region:** Users first define the printable area in the design tool based on their 3D printer’s build platform dimensions. The tool then displays a corresponding rectangle in Rhino’s workspace as a visual guide (Fig. 8.b).

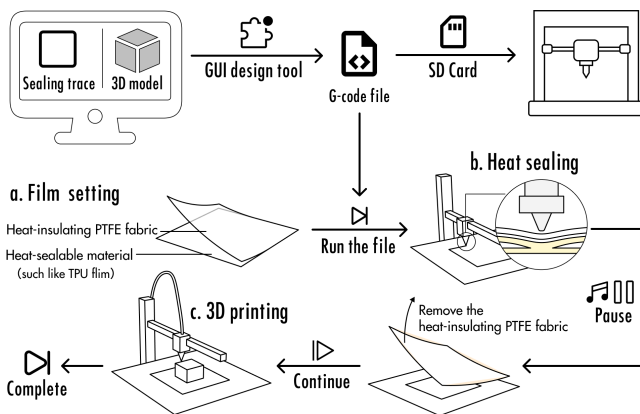


Figure 7: The overall fabrication pipeline.

- (2) **Complete the design:** Referring to DuoMorph’s design space, example primitives, and prior work [27, 47], users create heat-sealing patterns and 3D models of printed components in Rhino. If another modeling tool is used, the model can be imported into Rhino for the subsequent steps.
- (3) **Generate heat-sealing G-code:** After design completion, users select the heat-sealing pattern and fabric type in the tool (Fig. 8.a,b). The tool automatically converts the sketches into G-code. It samples the paths at 0.5 mm intervals and generates nozzle movements at speeds and heights optimized for the selected fabric. For multi-curve patterns, the nozzle lifts off the fabric between curves to avoid unwanted contact.
- (4) **Generate 3D printing G-code using general slicing software:** Users export the 3D components as STL files via the tool (Fig. 8.a,c) and slice them using standard third-party slicing software (e.g., Cura or Bambu Studio), which offers reliable settings for FDM printers. Because printing occurs directly on heat-sealed fabric, users must disable features like platform-based supports or brim that could damage the sealed areas. The tool will also generate an alignment marker in the STL to help position parts correctly in the slicing software (Fig. 8.c).
- (5) **Merge G-code:** Users return to the design tool and select the sliced 3D printing G-code. The tool automatically combines it with the heat-sealing G-code into a single file. A pause command and MIDI alert sound are inserted after the heat-sealing phase, allowing users to inspect sealing quality and prepare for printing (e.g., by removing heat-insulating PTFE fabric) before continuing.
- (6) **Export and run merged G-code:** Once merged, users can preview the complete G-code in the GUI, save it to a storage

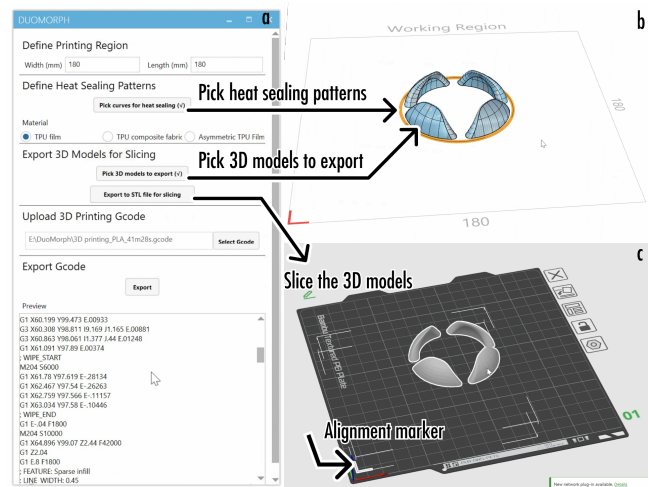
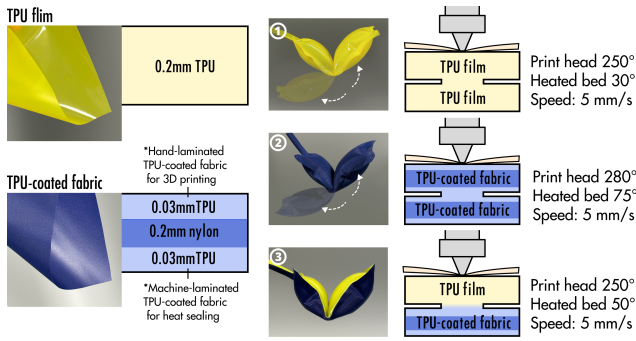


Figure 8: The design tool. (a) DuoMorph design tool GUI, which automatically (b) generates the G-code from sketches to fabricate the heat sealing patterns and (c) merges with the G-code for the 3D printing parts generated by general slicing software.



**Figure 9: Materials used for heat-sealing and corresponding settings.**

device (e.g., an SD card), transfer it to the 3D printer, and initiate the fabrication.

### 4.3 Heat Sealing Materials and Settings

**4.3.1 Material Selection.** Two commonly used sheet materials for making airbags are adopted in this research: a 0.2 mm TPU film (thermal conductivity  $\approx 0.2 \text{ W}/(\text{m}\cdot\text{K})$ ) and a 0.2 mm nylon fabric laminated with a 0.03 mm TPU layer (TPU-coated fabric, thermal conductivity  $\approx 0.25 \text{ W}/(\text{m}\cdot\text{K})$ ) (Fig. 9). The TPU film is softer and can therefore be more easily shaped by 4D-printed structures, whereas the TPU-coated fabric is stiffer and can better support printed structures when the airbag is not inflated. Note that most off-the-shelf coated fabrics are single-side laminated, and printed structures adhere poorly to bare nylon. For this reason, it is recommended to laminate the fabric surface intended for printing with an additional TPU film.

When the airbag is sealed using a single type of sheet material, it often, but not always, folds or bends toward the side in contact with the nozzle [27]. In contrast, when the two materials are combined,



**Figure 11: Qualitative adhesion performance.**

the airbag consistently deforms toward the TPU film side, owing to its softer and more stretchable nature.

**4.3.2 Heat-sealing Process (Fig. 10).** Based on the supplier’s recommendations, the nozzle temperature was set to 250 °C or 280 °C and the heated-bed temperature to 50 °C or 70 °C, both determined by the top-layer fabric. The print speed was fixed at 5 mm/s to ensure reliable heat sealing during printing (Fig. 9). In addition, a protective PTFE fabric (0.1mm thick, thermal conductivity:  $0.23 \text{ W}/(\text{m}\cdot\text{K})$ ) is applied when sealing TPU film to prevent scratching of the thin film. The PTFE fabric is as required for TPU-coated fabric to protect the coating. Finally, the force exerted during Z-axis homing at printer initialization is found to be sufficient for heat sealing, and therefore no additional press distance is specified in the G-code to increase force. Moreover, variations in film or fabric thickness can be accommodated by the homing process, eliminating any need for manual adjustment.

### 4.4 FDM Printing Filaments and Settings

**4.4.1 Filament Selection.** Three types of filament are used in this research: PLA (Bambu), TPU (Bambu), and TPU-based conductive filament (Qie feng). Among them, PLA and TPU are the most frequently applied. Structures printed with TPU generally exhibit stronger bonding with TPU films, owing to their chemical and mechanical compatibility (Fig. 11, left). Both TPU and PLA can adhere reasonably well to TPU-coated fabric, likely because the fabric layer reduces the elasticity compared to pure TPU film (Fig. 11, right).

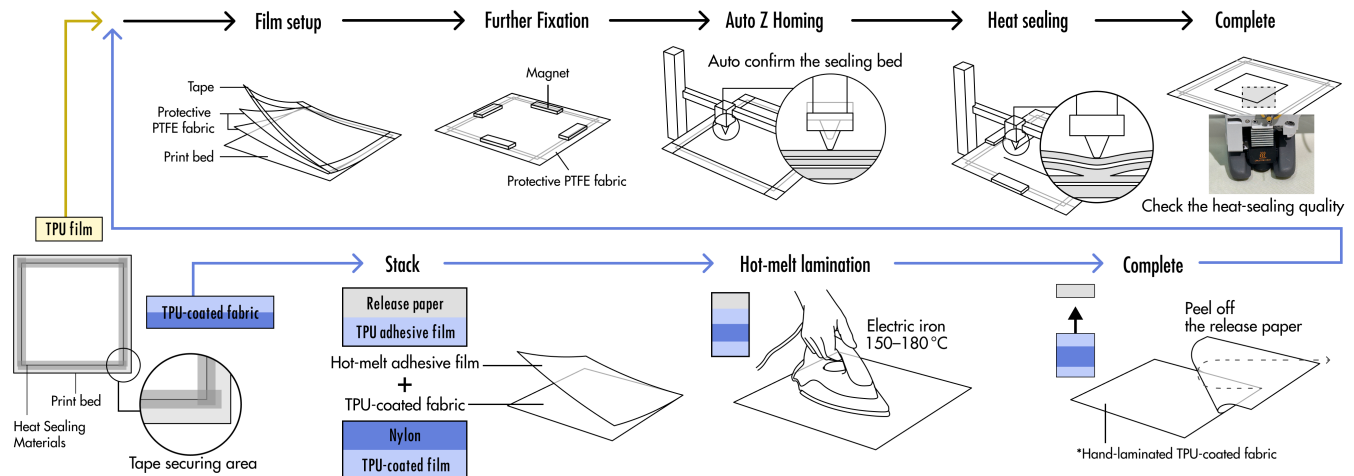


**Figure 10: The detailed workflow of heat-sealing.**

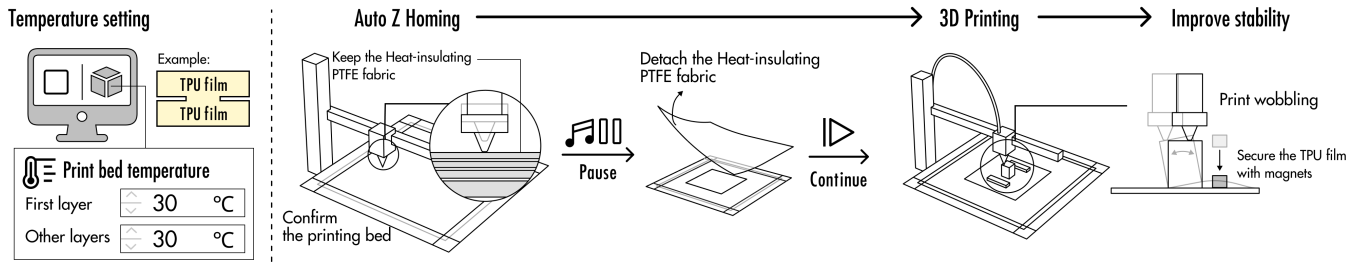


Figure 12: The detailed workflow for FDM printing.

Quantitative results of the bonding strength will be presented in Section 6.1. The conductive filament is primarily employed to introduce sensing capability.

**4.4.2 FDM process.** In this step (Fig. 12), a key difference from conventional 3D printing is that a heated print bed may soften the sheet materials—especially the TPU film—resulting in an unstable substrate and poor print quality. Therefore, it is recommended to keep the bed at room temperature (i.e., turn off bed heating), which our design tool automatically sets in the exported G-code. Except for setting the print bed temperature to 30 °C to prevent thermal deformation of the pneumatic actuator, all other parameters can follow the default recommendations of Bambu Studio for standard 3D printing. For 4D printing, configurations such as toolpath and print speed can be set according to previous work. [1, 40].

Another point of attention arises in 4D printing is, when printing structures for concave bending, it is advisable to add dissolvable supports for the arch, particularly when the span is large (Fig. 13). After printing, the support should first be dissolved in warm water (30–40 °C) before placing the structure in hot water to trigger deformation. Quantitative experiments to determine the optimal designs of the arch structures will be presented in Section 6.2. In addition, when the base of the arch structure in contact with the

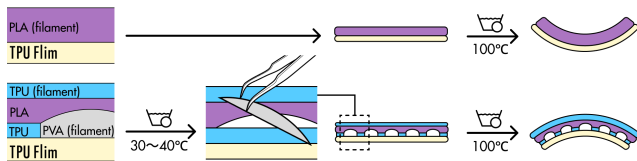


Figure 13: Additional treatment steps for 4D printing.

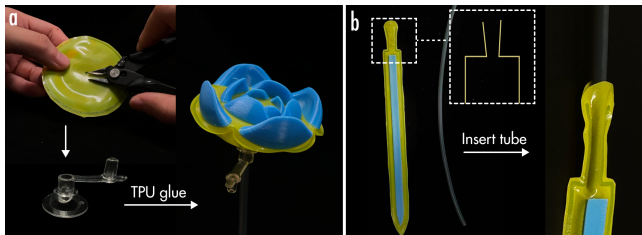


Figure 14: Two tubing assembly approaches.

sheet material is narrow, it is recommended to add a thin intermediate TPU layer to enhance the interfacial adhesion between the PLA arch and the sheet material.

### 4.5 Post-processing

After heat-sealing and printing, the actuator can be trimmed and the tubing manually assembled. The tubing can be assembled either vertically or horizontally. For vertical assembly (Fig. 14.a), a hole is cut in the actuator, and a valve is glued in place. The tube is then connected to the valve. Alternatively, if a channel was reserved during heat-sealing, the tube can simply be inserted horizontally and secured with adhesive (Fig. 14.b).

## 5 Applications

To demonstrate the potential of DuoMorph, we designed a set of application artifacts, including a kinetic sculpture, a biomimetic gripper, a desktop toy, and a massage neck pillow, each showcasing how different DuoMorph structures can be integrated to achieve expressive, functional, and interactive shape-changing interfaces.

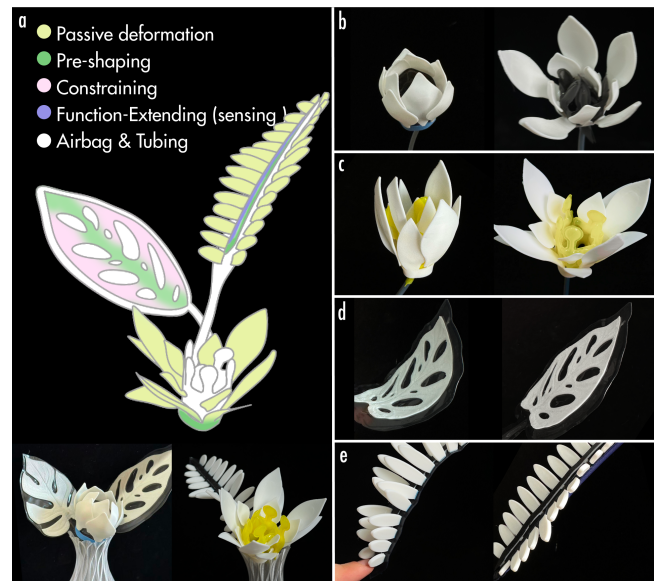


Figure 15: Kinetic sculpture integrating multiple types of DuoMorph structures.

## 5.1 Kinetic Sculpture

This example leverages all four types of printed structures to create plant-like kinetic sculptures that interact with visitors (Fig. 15.a). The flowers are equipped with 4D printed strips at their bases, allowing them to curl into cylinders when heated. The petals, printed directly on airbags, bloom when inflated (Fig. 15.b,c). A large leaf incorporates a 4D printed surface that bends the leaf after heated but flattens once the air chamber inflates (Fig. 15.d). The mimosa-inspired leaf integrates a 4D printed stem that curves a little bit to shape the leaf after heated and contains a sensing layer to detect human touch (Fig. 15.e). When touched, all airbags deflate, causing the mimosa leaves to fold, flowers to close, and large leaves to curve.

## 5.2 Biomimetic Gripper

This gripper is inspired by the Venus flytrap and is enabled by printed constraint, sensing, and friction-tuning structures (Fig. 16.a). A surface coating constrains air deformation when inflated, while dot-shaped protrusions increase friction during contact. In addition, spike-like structures printed with conductive PLA filament serve as sensors. As shown in Fig. 16.b, the gripper can respond to human touch. Moreover, when in contact with conductive objects (e.g., an aluminum foil ball), the sensors trigger the gripper to close around the object (Fig. 16.c).

## 5.3 Customized Massage Neck Pillow

This neck pillow (Fig. 17.a) is pre-shaped by a 4D-printed frame, which can be customized to the user's neck dimensions for optimal fit and conformity (Fig. 17.b,c). By embedding the geometric curvature directly into the 4D-printed structure, the pillow naturally aligns with the user's cervical contour without requiring continuous actuation. In addition, the 4D-printed frame offloads the shaping and support functions from the pneumatic actuator, allowing the actuator to focus exclusively on driving the inflation of the printed massage dots. This division of roles not only simplifies the actuator design but may also enhance the overall massage performance by enabling more targeted and consistent actuation.

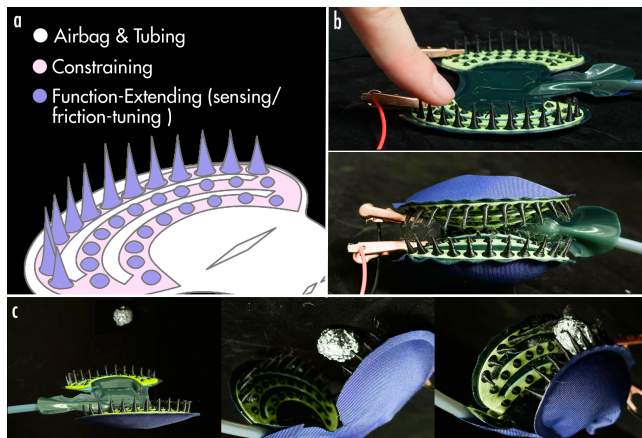


Figure 16: Biomimetic gripper inspired by *Dionaea muscipula* (Venus flytrap).

## 5.4 Desktop Toy

By integrating printed pre-shaping and passive deformation with pneumatic actuation, we created a hedgehog-inspired desktop toy (Fig. 18.a). The toy consists of two main components: an inner inflatable body and an outer 4D-printed shell that forms both the skin and the spines. When heated, the outer shell undergoes a programmed shape transformation, rolling into a cone-like geometry while the originally flat spines gently lift upward (Fig. 18.b). Once mounted on the inflated inner body, the shell can further expand, causing the spines to stand more prominently and enhancing the overall expressive effect. Through repeated inflation and deflation cycles, the toy produces rhythmic swaying and pulsating motions, giving rise to a playful, engaging interaction reminiscent of a small creature's breathing or movement (Fig. 18.c).

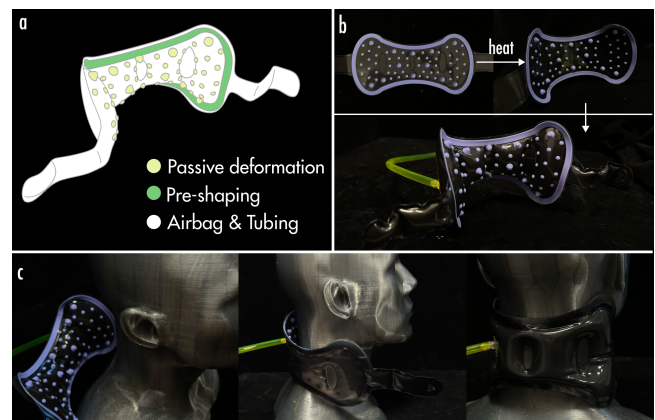


Figure 17: A customized neck pillow for Massage.

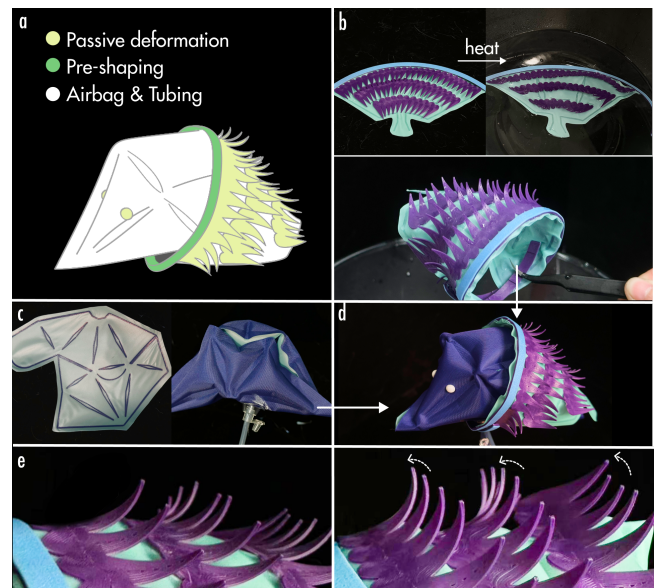


Figure 18: Hedgehog-inspired desktop toy demonstrating dynamic actuation.

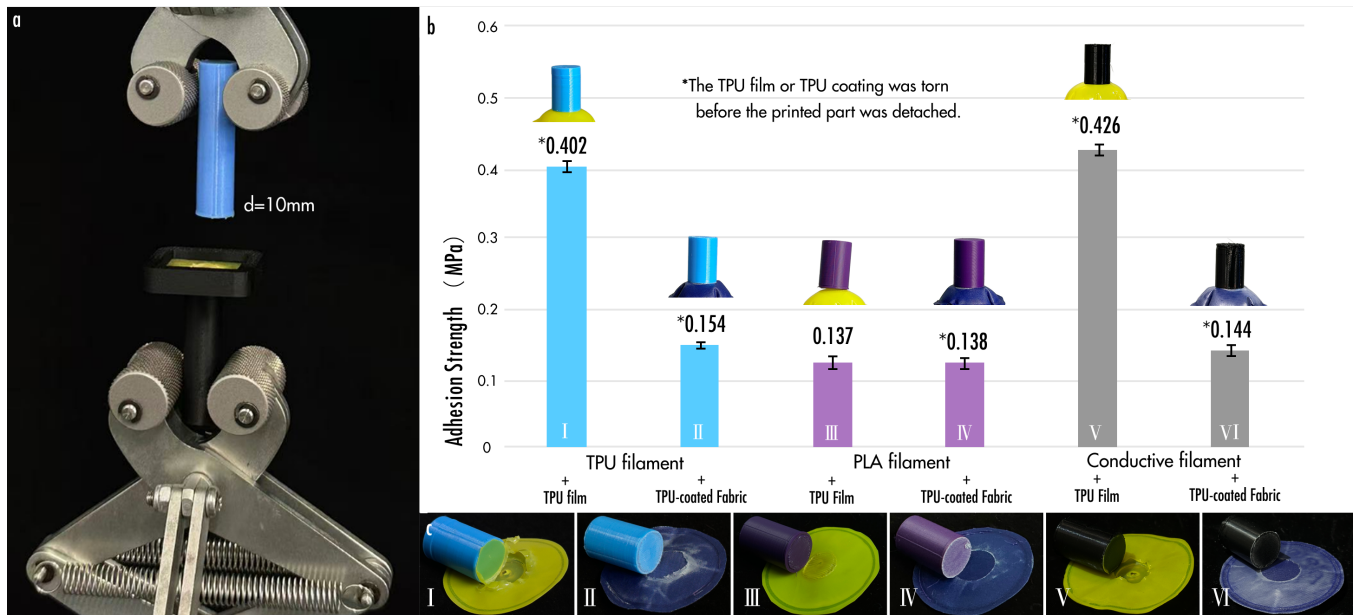


Figure 19: Tensile strength measurements for TPU film, TPU-coated fabric, and PLA/TPU combinations. (a) Test setup, (b) Test results, (c) post-separation contact surfaces across experimental groups.

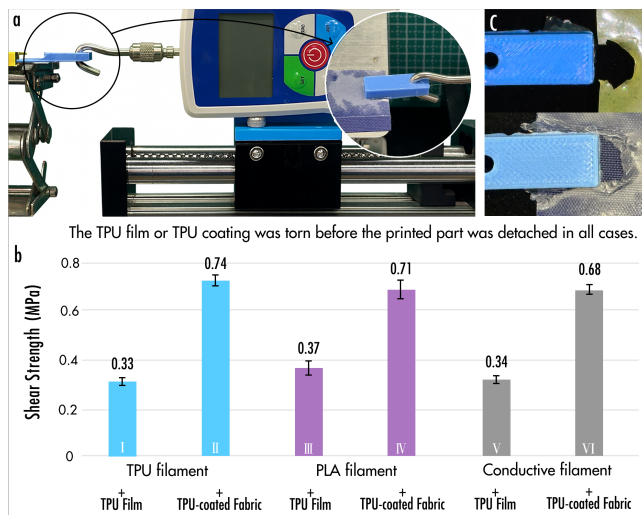


Figure 20: Shear strength measurements for TPU film, TPU-coated fabric, and PLA/TPU combinations. (a) Test setup, (b) Test results. (c) The TPU film and TPU coating were torn before the printed part was detached in all these six cases.

## 6 Evaluation

### 6.1 Adhesion Strength

The adhesion strength between printed structures and sheet materials is one of the most critical parameters in DuoMorph. To evaluate the tensile strength, we printed cylindrical samples (diameter: 10 mm, height: 40 mm) on different sheet materials vertically.

Then each combination was tested ten times using a universal testing machine. As shown in Fig. 19, TPU film combined with regular TPU filament and TPU-based conductive filament (groups i and v) exhibited the highest tensile strength. In fact, the actual bonding strength is even greater, as the TPU film itself ruptured prior to separation. In contrast, TPU film or coating combined with PLA filament (groups iii and iv) demonstrated the weakest tensile strength. And TPU-coated fabric combined with TPU filaments (groups ii and vi) also exhibited relatively low tensile strength due to the weaker adhesion between the hand-laminated TPU coating and the nylon substrate. These results indicate that materials of the same type exhibit significantly stronger interfacial adhesion, leading to improved mechanical performance.

Shear force tests were conducted using a shear force tester, as shown in Fig. 20.a. Thin brick-shaped samples (20 mm × 10 mm × 4 mm) were printed across the edge of different sheet materials, and each combination was tested ten times. Fig. 20.b shows the results. The actual shear strength will be even greater, as the TPU films or coatings ruptured before the printed parts detached in all six combinations (Fig. 20.c). This explains the similar results observed within groups i, iii, v and groups ii, iv, vi, which primarily reflect the force required to tear the TPU film or peel the TPU coating from the nylon substrate.

For TPU-coated fabric, which is originally single-sided, the TPU layer between the fabric and the filament was produced through manual lamination. Although the manually laminated TPU layer was thin (0.03 mm), the TPU filament penetrated into the woven nylon gaps during thermal pressindue to minor plastic deformation, forming both micro-mechanical interlocks and molecular-level wetting. As a result, the adhesion strength was higher for both TPU and PLA printed structures compared to plain TPU film.

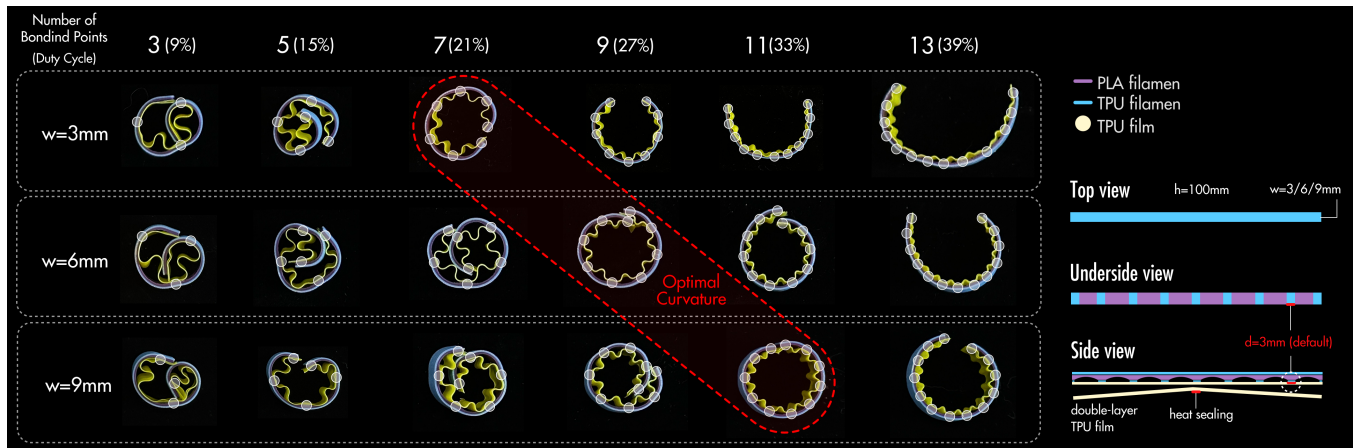


**Figure 21: Bending curvature results under different strip widths and bonding ratios. Red dashed line marks optimal circular bending.**

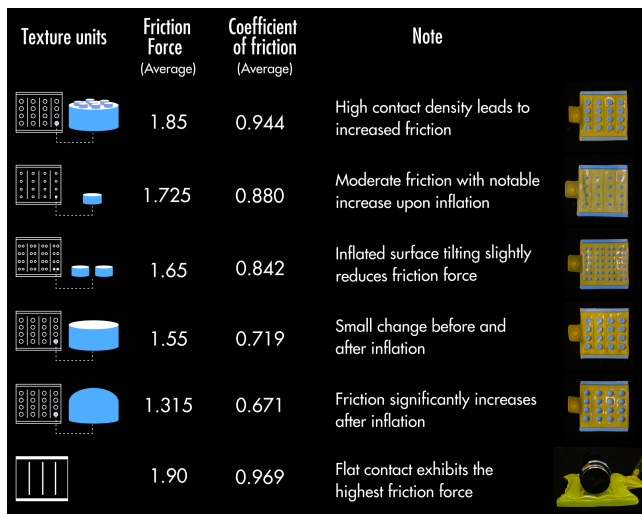


**Figure 22: Comparison of friction coefficients for different printed surface textures and structures.**

## 6.2 Concave Bending in 4D Printing

To investigate factors affecting concave bending curvature, we prepared three sets of samples (widths: 3, 6, and 9 mm; length: 100 mm) printed on double-layer TPU films. For each width, six bonding ratio patterns (bonding point width: 3 mm) were tested to analyze the relationship between bonded area and curvature. Other variables such as water temperature (100°C), material, and fabrication process were kept constant.

As shown in Fig. 21, the results indicate:

- (1) Lower bonding ratios (larger unbonded regions) produced stronger bending, until limited by the curling stiffness of the TPU film.
- (2) At the same bonding ratio, wider strips resulted in greater curvature.

- (3) The optimal bending condition (approximating a closed circle, marked with a red dashed line) followed a diagonal trend: as width increased, the required number of bonding points also increased to maintain similar bending efficiency.

In summary, for large-area pneumatic actuators, wider concave-bending strips are recommended to enhance curvature. For small-area actuators, the design can be tuned more flexibly:

- To achieve strong curvature, use low bonding ratios or wider strips.
- To achieve mild curvature, use high bonding ratios or narrower strips.
- To form a near-perfect circular arc, select the appropriate combination of width and bonding ratio along the optimal curvature trend.

## 6.3 Friction Tunability

We also evaluated how different surface patterns influence frictional performance (results shown in Fig. 22). All samples are fully inflated and is tested with a 200g weight loaded. In general, adding printed textures reduced the measured coefficient of friction, likely due to decreased effective contact area. Alternatively, other type geometries—such as flat surface patches or suction-cup-like features—might significantly increase friction and adhesion. These results highlight the design flexibility of Duomorph in tailoring surface interaction properties for specific applications.

## 7 Limitations, Discussion, and Future Work

**Single-Sided Printing.** In the current workflow, structures can only be printed on one side of the airbag, which introduces constraints that must be carefully considered during the design phase. For example, achieving convex 4D bending requires specifically designed bases to redirect the deformation to the printable side. Another strategy is to leverage modular connectors so that multiple prototypes can be joined back-to-back, enabling both sides of the combined structure to host functional features.

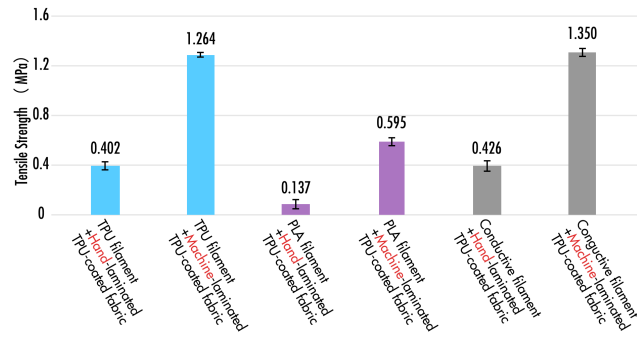


**Figure 23: Adhesion strength comparison between manually coated and industrially coated double-sided TPU fabrics.**

**Printing Height Limits on Unstable Substrates.** Replacing the conventional rigid build plate with a soft film introduces challenges in height control. During printing, deformation of the flexible substrate can cause vertical displacement, leading to misaligned layers or nozzle collisions. This issue is particularly evident when using TPU film as the actuator material, as heating or pressure changes can lift the surface. (In contrast, TPU-coated fabric, due to its stiffness, shows minimal height variation.) To mitigate this, we fixed the actuator to the platform with double-sided tape to suppress displacement and reduced print speed to lower mechanical impact. With these measures, we successfully printed TPU filaments up to 7 cm tall on TPU film substrates. Looking ahead, vacuum-based clamping systems specialized for thin-film materials (e.g., [15]) could be adapted to clamp the films to further stabilize the process.

**Improved Double-Sided TPU-Coated Fabric.** Most commercially available TPU-coated fabrics are single-side coated, requiring manual lamination of an extra TPU layer before FDM printing (since nylon surfaces are non-adhesive to printed polymers). Heat pressing or ironing TPU film onto textiles is possible, but manual coating is highly quality-sensitive: trapped air pockets or uneven pressure often produce weak bonds prone to delamination during printing. To overcome this, we sourced machine-laminated double-sided TPU-coated fabrics (~0.5 mm thick, about twice the thickness of the single-sided variant we currently use). In a comparative tensile strength test, the bonding strength with TPU filament increased by approximately 3.2 times, while that with PLA filament increased by about 4.3 times (Fig. 23).

**Structural Reinforcement via Weaving.** During our research, we found that TPU filament exhibits superior interfacial bonding with TPU film, and is therefore often used as the first printed layer to improve adhesion of rigid filaments such as PLA. However, simple layer stacking remains vulnerable to delamination under concentrated stress. To address this, we propose weaving-inspired reinforcement: interlacing print paths or embedding interlocking regions to create mechanical interlocks across layers and interfaces. This strategy has the potential to enhance tensile and shear resistance, leading to stronger and more durable hybrid structures.

**Multi-material support, generalization and durability.** Compared to SLA printing, FDM printing presents a lower barrier for

multi-material fabrication and, by nature, SLA does not support heat sealing. In this work, we explore two types of fabrics combined with a range of printing filaments, enabling varied bonding outcomes. Empirically, materials with similar properties tend to exhibit stronger adhesion. Prior studies [4, 24] have begun to explore FDM-based thermal bonding; however, they still present minor issues, such as uneven finished surface. DuoMorph advances heat-sealing quality by incorporating a protective PTFE fabric, achieving stable and smooth thermal bonding with FDM printers. This smooth and reliable bonding surface further supports high-quality subsequent FDM printing directly onto the fabric. These efforts make the technology theoretically more generalizable across different FDM printers. In addition, durability tests demonstrate excellent performance of DuoMorph prototypes. The airtightness of the seams is outstanding: TPU-film-based airbags ruptured at the film before seam failure, while TPU-coated fabric airbags withstood the maximum air pressure of the testing machine without leakage. In another test, samples underwent 1,000 inflation-deflation cycles and remained fully functional, with no detachment of printed structures and no leakage. Detailed results are provided in the Appendix.

## 8 Conclusion

In this work, we introduced *DuoMorph*, a design and fabrication approach that integrates FDM printing with pneumatic actuation to realize novel shape-changing interfaces. By co-designing printed structures and heat-sealed pneumatic elements, DuoMorph enables actuation and constraint mechanisms that are difficult for either modality to achieve alone. Importantly, the entire hybrid structure can be produced in a single, seamless workflow using a standard FDM printer, encompassing both heat-sealing and 3D/4D printing. We formalized the design space through four primitive categories that characterize the fundamental modes of interaction between printed and pneumatic components. In addition, we developed a fabrication method and supporting design tool to operationalize this process. Through example applications and performance demonstrations, we showcased the versatility and expressive potential of DuoMorph, ranging from kinetic sculptures and biomimetic grippers to playful interactive artifacts and functional neck pillows. Together, these contributions establish DuoMorph as a new pathway for creating hybrid material systems that expand the possibilities of shape-changing interfaces, and lay the groundwork for future explorations in responsive, functional, and interactive design.

## Acknowledgments

We acknowledge Hengrong Ni’s assistance with rapid early-stage validation when the core concept was first proposed by Dr. Lu. We thank the MiLab at Tsinghua University for its support, and Prof. Huirong Le of The Future Laboratory for providing equipment for performance evaluation. Special thanks go to Tingyu Hua from Prof. Le’s team for his assistance with the tests. We also thank Jeremy Chen from the Morphing Matter Lab for his early coding support. This work was supported by the PolyU Strategic Hiring Scheme (Project P0059979) and partially by the U.S. National Science Foundation (Award No. 2427455).

## References

- [1] Byoungkwon An, Ye Tao, Jianzhe Gu, Tingyu Cheng, Xiang 'Anthony' Chen, Xiaoxiao Zhang, Wei Zhao, Youngwook Do, Shigeo Takahashi, Hsiang-Yun Wu, Teng Zhang, and Lining Yao. 2018. Thermorph: Democratizing 4D Printing of Self-Folding Materials and Interfaces. In *Proceedings of the 2018 CHI Conference on Human Factors in Computing Systems*. ACM, Montreal QC Canada, 1–12. doi:10.1145/3173574.3173834
- [2] Robert L. Baines, Sree Kalyan Patiballa, and Rebecca Kramer-Bottiglio. 2021. Rapidly Reconfigurable Inextensible Inflatables. In *2021 IEEE 4th International Conference on Soft Robotics (RoboSoft)*. 29–34. doi:10.1109/RoboSoft51838.2021.9479435
- [3] Yu-Wen Chen, Wei-Ju Lin, Yi Chen, and Lung-Pan Cheng. 2021. PneuSeries: 3D Shape Forming with Modularized Serial-Connected Inflatables. In *The 34th Annual ACM Symposium on User Interface Software and Technology*. ACM, Virtual Event USA, 431–440. doi:10.1145/3472749.3474760
- [4] Kyung Yun Choi and Hiroshi Ishii. 2021. Therms-Up!: DIY Inflatables and Interactive Materials by Upcycling Wasted Thermoplastic Bags. In *Proceedings of the Fifteenth International Conference on Tangible, Embedded, and Embodied Interaction (TEI '21)*. Association for Computing Machinery, New York, NY, USA, 1–8. doi:10.1145/3430524.3442457
- [5] Kyung Yun Choi, Jimmo Lee, Neska ElHaouij, Rosalind Picard, and Hiroshi Ishii. 2021. aSpire: Clippable, Mobile Pneumatic-Haptic Device for Breathing Rate Regulation via Personalizable Tactile Feedback. In *Extended Abstracts of the 2021 CHI Conference on Human Factors in Computing Systems (CHI EA '21)*. Association for Computing Machinery, New York, NY, USA, 1–8. doi:10.1145/3411763.3451602
- [6] Colter J. Decker, Haihui Joy Jiang, Markus P. Nemitz, Samuel E. Root, Anoop Rajappan, Jonathan T. Alvarez, Giovanna Tracz, Lukas Wille, Daniel J. Preston, and George M. Whitesides. 2022. Programmable soft valves for digital and analog control. *Proceedings of the National Academy of Sciences* 119, 40 (Oct. 2022), e2205922119. doi:10.1073/pnas.2205922119 Publisher: Proceedings of the National Academy of Sciences.
- [7] Alexandra Delazio, Ken Nakagaki, Roberta L. Klatzky, Scott E. Hudson, Jill Fain Lehman, and Alanson P. Sample. 2018. Force Jacket: Pneumatically-Actuated Jacket for Embodied Haptic Experiences. In *Proceedings of the 2018 CHI Conference on Human Factors in Computing Systems (CHI '18)*. Association for Computing Machinery, New York, NY, USA, 1–12. doi:10.1145/3173574.3173894
- [8] Sean Follmer, Daniel Leithinger, Alex Olwal, Nadia Cheng, and Hiroshi Ishii. 2012. Jamming user interfaces: programmable particle stiffness and sensing for malleable and shape-changing devices. In *Proceedings of the 25th annual ACM symposium on User interface software and technology (UIST '12)*. Association for Computing Machinery, New York, NY, USA, 519–528. doi:10.1145/2380116.2380181
- [9] Jack Forman, Mustafa Doga Dogan, Hamilton Forsythe, and Hiroshi Ishii. 2020. DefeXtiles: 3D Printing Quasi-Woven Fabric via Under-Extrusion. In *Proceedings of the 33rd Annual ACM Symposium on User Interface Software and Technology (UIST '20)*. Association for Computing Machinery, New York, NY, USA, 1222–1233. doi:10.1145/3379337.3415876
- [10] Jianzhe Gu, Yuyu Lin, Qiang Cui, Xiaoqian Li, Jiayi Li, Lingyun Sun, Cheng Yao, Fangtian Ying, Guanyun Wang, and Lining Yao. 2022. PneuMesh: Pneumatic-driven Truss-based Shape Changing System. In *Proceedings of the 2022 CHI Conference on Human Factors in Computing Systems (CHI '22)*. Association for Computing Machinery, New York, NY, USA, 1–12. doi:10.1145/3491102.3502099
- [11] Liang He, Cheng Xu, Ding Xu, and Ryan Brill. 2015. PneuHaptic: delivering haptic cues with a pneumatic armband. In *Proceedings of the 2015 ACM International Symposium on Wearable Computers (ISWC '15)*. Association for Computing Machinery, New York, NY, USA, 47–48. doi:10.1145/2802083.2802091
- [12] Donal Padraic Holland, Colette Abah, Marielena Velasco-Enriquez, Maxwell Herman, Gareth J. Bennett, Emir Augusto Vela, and Conor James Walsh. 2017. The Soft Robotics Toolkit: Strategies for Overcoming Obstacles to the Wide Dissemination of Soft-Robotic Hardware. *IEEE Robotics & Automation Magazine* 24, 1 (March 2017), 57–64. doi:10.1109/MRA.2016.2639067
- [13] Hyunyoung Kim, Aluna Everitt, Carlos Tejada, Mengyu Zhong, and Daniel Ashbrook. 2021. MorpheesPlug: A Toolkit for Prototyping Shape-Changing Interfaces. In *Proceedings of the 2021 CHI Conference on Human Factors in Computing Systems*. ACM, Yokohama Japan, 1–13. doi:10.1145/3411764.3445786
- [14] Christopher Kopic and Kristian Gohlke. 2016. InflatIBits: A Modular Soft Robotic Construction Kit for Children. In *Proceedings of the TEI '16: Tenth International Conference on Tangible, Embedded, and Embodied Interaction (TEI '16)*. Association for Computing Machinery, New York, NY, USA, 723–728. doi:10.1145/2839462.2872962
- [15] Qiuyu Lu, Jifei Ou, João Wilbert, André Haben, Haipeng Mi, and Hiroshi Ishii. 2019. milliMorph – Fluid-Driven Thin Film Shape-Change Materials for Interaction Design. In *Proceedings of the 32nd Annual ACM Symposium on User Interface Software and Technology (UIST '19)*. Association for Computing Machinery, New York, NY, USA, 663–672. doi:10.1145/3332165.3347956
- [16] Qiuyu Lu, Jifei Ou, Lining Yao, and Hiroshi Ishii. 2024. milleCrepe: Extending Capabilities of Fluid-driven Interfaces with Multilayer Structures and Diverse Actuation Media. In *Extended Abstracts of the CHI Conference on Human Factors in Computing Systems (CHI EA '24)*. Association for Computing Machinery, New York, NY, USA, 1–10. doi:10.1145/3613905.3650891
- [17] Qiuyu Lu, Haiqing Xu, Yijie Guo, Joey Yu Wang, and Lining Yao. 2023. Fluidic Computation Kit: Towards Electronic-free Shape-changing Interfaces. In *Proceedings of the 2023 CHI Conference on Human Factors in Computing Systems (CHI '23)*. Association for Computing Machinery, New York, NY, USA, 1–21. doi:10.1145/3544548.3580783
- [18] Qiuyu Lu, Tianyu Yu, Semina Yi, Yuran Ding, Haipeng Mi, and Lining Yao. 2023. SustainInflatable: Harvesting, Storing and Utilizing Ambient Energy for Pneumatic Morphing Interfaces. In *Proceedings of the 36th Annual ACM Symposium on User Interface Software and Technology (UIST '23)*. Association for Computing Machinery, New York, NY, USA, 1–20. doi:10.1145/3586183.3606721
- [19] Yiyue Luo, Kui Wu, Andrew Spielberg, Michael Foshey, Daniela Rus, Tomás Palacios, and Wojciech Matusik. 2022. Digital Fabrication of Pneumatic Actuators with Integrated Sensing by Machine Knitting. In *Proceedings of the 2022 CHI Conference on Human Factors in Computing Systems (CHI '22)*. Association for Computing Machinery, New York, NY, USA, 1–13. doi:10.1145/3491102.3517577
- [20] Li-Ke Ma, Yizhong Zhang, Yang Liu, Kun Zhou, and Xin Tong. 2017. Computational design and fabrication of soft pneumatic objects with desired deformations. *ACM Trans. Graph.* 36, 6 (Nov. 2017), 239:1–239:12. doi:10.1145/3130800.3130850
- [21] Farhang Momeni, Seyed M. Mehdi Hassani, N. Xun Liu, and Jun Ni. 2017. A review of 4D printing. *Materials & Design* 122 (May 2017), 42–79. doi:10.1016/j.matdes.2017.02.068
- [22] Hedieh Moradi and César Torres. 2020. Siloseam: A Morphogenetic Workflow for the Design and Fabrication of Inflatable Silicone Bladders. In *Proceedings of the 2020 ACM Designing Interactive Systems Conference (DIS '20)*. Association for Computing Machinery, New York, NY, USA, 1995–2006. doi:10.1145/3357236.3395473 event-place: Eindhoven, Netherlands.
- [23] Takafumi Morita, Ziyuan Jiang, Kanon Aoyama, Ayato Minaminosono, Yu Kuwajima, Naoki Hosoya, Shingo Maeda, and Yasuaki Kakehi. 2023. InflatableMod: Untethered and Reconfigurable Inflatable Modules for Tabletop-sized Pneumatic Physical Interfaces. In *Proceedings of the 2023 CHI Conference on Human Factors in Computing Systems*. ACM, Hamburg Germany, 1–15. doi:10.1145/3544548.3581353
- [24] Tom Morrison. 2020. Fusing Plastic Sheets With a 3D Printer... Sort Of. <https://hackaday.com/2020/05/14/fusing-plastic-sheets-with-a-3d-printer-sort-of/>. Accessed: 2025-11-17.
- [25] Ryuma Niiyama, Xu Sun, Lining Yao, Hiroshi Ishii, Daniela Rus, and Sangbae Kim. 2015. Sticky Actuator: Free-Form Planar Actuators for Animated Objects. In *Proceedings of the Ninth International Conference on Tangible, Embedded, and Embodied Interaction (TEI '15)*. Association for Computing Machinery, New York, NY, USA, 77–84. doi:10.1145/2677199.2680600
- [26] Jifei Ou, Felix Heibeck, and Hiroshi Ishii. 2016. TEI 2016 Studio: Inflated Curiosity. *MIT web domain* (Feb. 2016). <https://dspace.mit.edu/handle/1721.1/113823> Accepted: 2018-02-20T14:50:39Z ISBN: 9781450335829 Publisher: Association for Computing Machinery.
- [27] Jifei Ou, Mélina Skouras, Nikolaos Vlavianos, Felix Heibeck, Chin-Yi Cheng, Jannik Peters, and Hiroshi Ishii. 2016. aeroMorph - Heat-sealing Inflatable Shape-change Materials for Interaction Design. In *Proceedings of the 29th Annual Symposium on User Interface Software and Technology (UIST '16)*. Association for Computing Machinery, New York, NY, USA, 121–132. doi:10.1145/2984511.2984520
- [28] Mehmet Ozdemir, Marwa AlAlawi, Mustafa Doga Dogan, J. F. Martinez Castro, Stefanie Mueller, and E. L. Doubrovski. 2024. Speed-Modulated Ironing: High-Resolution Shade and Texture Gradients in Single-Material 3D Printing. In *Proceedings of the 37th Annual ACM Symposium on User Interface Software and Technology (UIST '24)*. ACM, Pittsburgh, PA, USA, 1–12. doi:10.1145/3654777.3676456
- [29] Sergio Picella, Catharina M. van Riet, and Johannes T. B. Overvelde. 2024. Pneumatic coding blocks enable programmability of electronics-free fluidic soft robots. *Science Advances* 10, 51 (Dec. 2024), eadr2433. doi:10.1126/sciadv.adr2433 Publisher: American Association for the Advancement of Science.
- [30] Daniela Rus and Michael T. Tolley. 2015. Design, fabrication and control of soft robots. *Nature* 521, 7553 (May 2015), 467–475. doi:10.1038/nature14543
- [31] Harpreet Sareen, Udayan Umaphathi, Patrick Shin, Yasuaki Kakehi, Jifei Ou, Hiroshi Ishii, and Pattie Maes. 2017. PrintInflatables: Printing Human-Scale, Functional and Dynamic Inflatable Objects. In *Proceedings of the 2017 CHI Conference on Human Factors in Computing Systems*. ACM, Denver Colorado USA, 3669–3680. doi:10.1145/3025453.3025898
- [32] Valkyrie Savage, Carlos Tejada, Mengyu Zhong, Raf Ramakers, Daniel Ashbrook, and Hyunyoung Kim. 2022. AirLogic: Embedding Pneumatic Computation and I/O in 3D Models to Fabricate Electronics-Free Interactive Objects. In *Proceedings of the 35th Annual ACM Symposium on User Interface Software and Technology*. ACM, Bend OR USA, 1–12. doi:10.1145/3526113.3545642
- [33] Ali Shtarbanov. 2021. FlowIO Development Platform – the Pneumatic “Raspberry Pi” for Soft Robotics. In *Extended Abstracts of the 2021 CHI Conference on Human Factors in Computing Systems (CHI EA '21)*. Association for Computing Machinery, New York, NY, USA, 1–6. doi:10.1145/3411763.3451513
- [34] Haruki Takahashi and Jeeun Kim. 2019. 3D Printed Fabric: Techniques for Design and 3D Weaving Programmable Textiles. In *Proceedings of the 32nd Annual ACM*

- Symposium on User Interface Software and Technology (UIST '19)*. Association for Computing Machinery, New York, NY, USA, 43–51. doi:10.1145/3332165.3347896
- [35] Haruki Takahashi and Homei Miyashita. 2017. Expressive Fused Deposition Modeling by Controlling Extruder Height and Extrusion Amount. In *Proceedings of the 2017 CHI Conference on Human Factors in Computing Systems (CHI '17)*. Association for Computing Machinery, New York, NY, USA, 5065–5074. doi:10.1145/3025453.3025933
- [36] Shan-Yuan Teng, Tzu-Sheng Kuo, Chi Wang, Chi-huan Chiang, Da-Yuan Huang, Liwei Chan, and Bing-Yu Chen. 2018. PuPoP: Pop-up Prop on Palm for Virtual Reality. In *Proceedings of the 31st Annual ACM Symposium on User Interface Software and Technology*. ACM, Berlin Germany, 5–17. doi:10.1145/3242587.3242628
- [37] Yingjun Tian, Renbo Su, Xilong Wang, Nur Banu Altin, Guoxin Fang, and Charlie C. L. Wang. 2023. OpenPneu: Compact Platform for Pneumatic Actuation with Multi-Channels. In *2023 IEEE/ASME International Conference on Advanced Intelligent Mechatronics (AIM)*. 765–770. doi:10.1109/AIM46323.2023.10196254 ISSN: 2159-6255.
- [38] Marynel Vázquez, Eric Brockmeyer, Ruta Desai, Chris Harrison, and Scott E. Hudson. 2015. 3D Printing Pneumatic Device Controls with Variable Activation Force Capabilities. In *Proceedings of the 33rd Annual ACM Conference on Human Factors in Computing Systems (CHI '15)*. Association for Computing Machinery, New York, NY, USA, 1295–1304. doi:10.1145/2702123.2702569
- [39] Guanyun Wang, Junzhe Ji, Yunkai Xu, Lei Ren, Xiaoyang Wu, Chunyuan Zheng, Xiaojing Zhou, Xin Tang, Boyu Feng, Lingyun Sun, Ye Tao, and Jiayi Li. 2024. X-Hair: 3D Printing Hair-like Structures with Multi-form, Multi-property and Multi-function. In *Proceedings of the 37th Annual ACM Symposium on User Interface Software and Technology (UIST '24)*. Association for Computing Machinery, New York, NY, USA, 1–14. doi:10.1145/3654777.3676360
- [40] Guanyun Wang, Ye Tao, Ozguc Bertug Capunaman, Humphrey Yang, and Lining Yao. 2019. A-line: 4D Printing Morphing Linear Composite Structures. In *Proceedings of the 2019 CHI Conference on Human Factors in Computing Systems (CHI '19)*. Association for Computing Machinery, New York, NY, USA, 1–12. doi:10.1145/3290605.3300656
- [41] Guanyun Wang, Humphrey Yang, Zeyu Yan, Nurcan Gecer Ulu, Ye Tao, Jianzhe Gu, Levent Burak Kara, and Lining Yao. 2018. 4DMesh: 4D Printing Morphing Non-Developable Mesh Surfaces. In *Proceedings of the 31st Annual ACM Symposium on User Interface Software and Technology (UIST '18)*. Association for Computing Machinery, New York, NY, USA, 623–635. doi:10.1145/3242587.3242625
- [42] Guanyun Wang, Kuangqi Zhu, Lingchuan Zhou, Mengyan Guo, Haotian Chen, Zihan Yan, Deying Pan, Yue Yang, Jiayi Li, Jiang Wu, Ye Tao, and Lingyun Sun. 2023. PneuFab: Designing Low-Cost 3D-Printed Inflatable Structures for Blow Molding Artifacts. In *Proceedings of the 2023 CHI Conference on Human Factors in Computing Systems*. ACM, Hamburg Germany, 1–17. doi:10.1145/3544548.3580923
- [43] Matheus S. Xavier, Charbel D. Tawk, Yuen K. Yong, and Andrew J. Fleming. 2021. 3D-printed omnidirectional soft pneumatic actuators: Design, modeling and characterization. *Sensors and Actuators A: Physical* 332 (Dec. 2021), 113199. doi:10.1016/j.sna.2021.113199
- [44] Junichi Yamaoka, Ryuma Niiyama, and Yasuaki Kakehi. 2017. BlowFab: Rapid Prototyping for Rigid and Reusable Objects using Inflation of Laser-cut Surfaces. In *Proceedings of the 30th Annual ACM Symposium on User Interface Software and Technology*. ACM, Québec City QC Canada, 461–469. doi:10.1145/3126594.3126624
- [45] Junichi Yamaoka, Kazunori Nozawa, Shion Asada, Ryuma Niiyama, Yoshihiro Kawahara, and Yasuaki Kakehi. 2018. AccordionFab: Fabricating Inflatable 3D Objects by Laser Cutting and Welding Multi-Layered Sheets. In *Adjunct Proceedings of the 31st Annual ACM Symposium on User Interface Software and Technology*. ACM, Berlin Germany, 160–162. doi:10.1145/3266037.3271636
- [46] Zeyu Yan and Huaishu Peng. 2021. FabHydro: Printing Interactive Hydraulic Devices with an Affordable SLA 3D Printer. In *The 34th Annual ACM Symposium on User Interface Software and Technology*. ACM, Virtual Event USA, 298–311. doi:10.1145/3472749.3474751
- [47] Yue Yang, Lei Ren, Chuang Chen, Bin Hu, Zhuoyi Zhang, Xinyan Li, Yanchen Shen, Kuangqi Zhu, Junzhe Ji, Yuyang Zhang, Yongbo Ni, Jiayi Wu, Qi Wang, Jiang Wu, Lingyun Sun, Ye Tao, and Guanyun Wang. 2024. SnapInflatables: Designing Inflatables with Snap-through Instability for Responsive Interaction. In *Proceedings of the CHI Conference on Human Factors in Computing Systems*. ACM, Honolulu HI USA, 1–15. doi:10.1145/3613904.3642933
- [48] Lining Yao, Ryuma Niiyama, Jifei Ou, Sean Follmer, Clark Della Silva, and Hiroshi Ishii. 2013. PneuUI: pneumatically actuated soft composite materials for shape changing interfaces. In *Proceedings of the 26th annual ACM symposium on User interface software and technology*. ACM, St. Andrews Scotland, United Kingdom, 13–22. doi:10.1145/2501988.2502037
- [49] Hye Jun Youn and Ali Shtarbanov. 2022. PneuBots: Modular Inflatables for Playful Exploration of Soft Robotics. In *CHI Conference on Human Factors in Computing Systems Extended Abstracts*. ACM, New Orleans LA USA, 1–6. doi:10.1145/3491101.3514490
- [50] Tianyu Yu, Mengjia Niu, Haipeng Mi, and Qiuyu Lu. 2024. MilliWare: Parametric Modeling and Simulation of Millifluidic Shape-changing Interface. In *Proceedings of the Eleventh International Symposium of Chinese CHI (Denpasar, Bali, Indonesia) (CHCHI '23)*. Association for Computing Machinery, New York, NY, USA, 461–467. doi:10.1145/3629606.3629654
- [51] Xiaoliang Zhao, Jia Chen, Jinhui Li, Mengmeng Jin, Zihan Deng, Xiaopeng Li, Wei Zhang, Minghua Jin, Fangtian Ying, Qi Wang, and Guanyun Wang. 2022. MultiPneu: Inflatable Deformation of Multilayered Film Materials. In *Proceedings of the Ninth International Symposium of Chinese CHI (Chinese CHI '21)*. Association for Computing Machinery, New York, NY, USA, 158–161. doi:10.1145/3490355.3490517

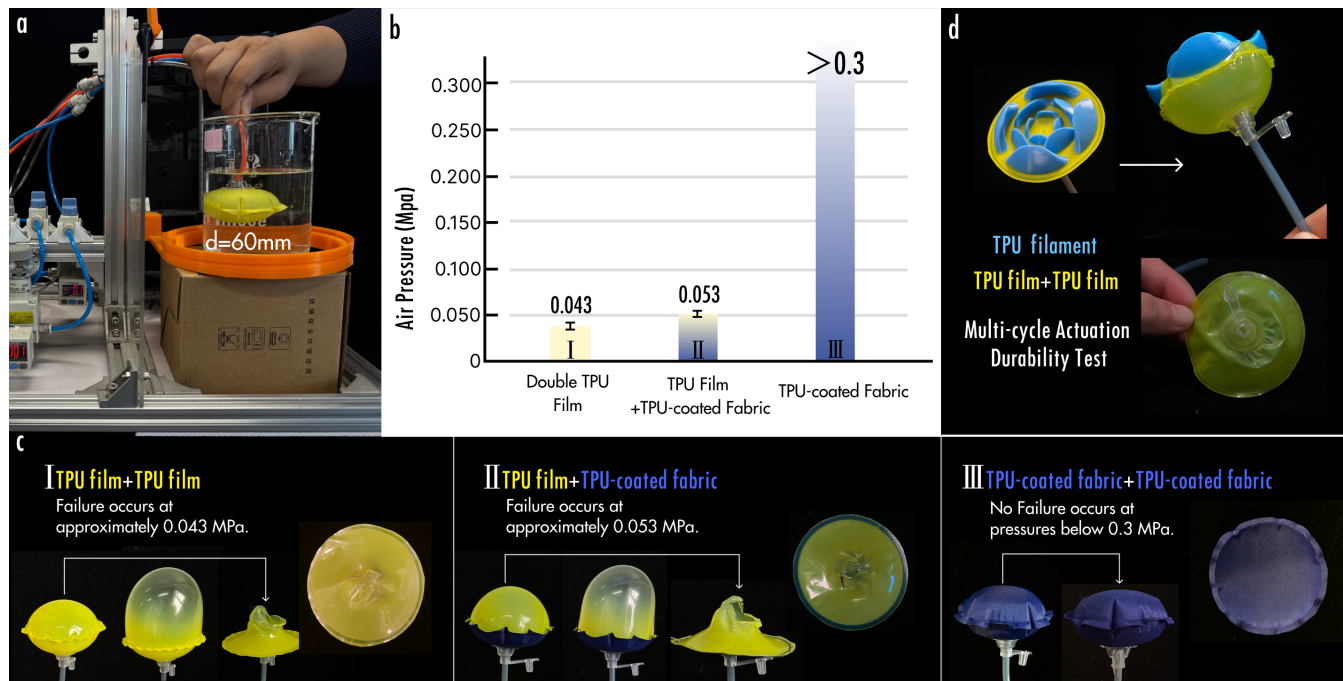


Figure 24: Airtightness and reusability experiments. (a) Test setup, (b) Airtightness test results, (c) Tested airtightness sample details, (d) A tested reusability sample details.

## A Durability Test

### A.1 Airtightness

The airtightness of three types of pneumatic actuators, fabricated by combining two types of film/fabric, was tested using the setup shown in Fig. 24.a. Air leakage was detected through visual observation of bubbles and by monitoring the air pressure drop. As illustrated in Fig. 24.b and c, Groups 1 and 2 failed due to rupture of the TPU film rather than seam failure, whereas Group 3 withstood the maximum air pressure of the testing machine without leakage.

### A.2 Reusability

Reusability was primarily evaluated by repeatedly inflating and deflating 6 cm-diameter pneumatic actuators made of TPU film with petal-shaped 3D-printed structures (Fig. 24.d), for 1,000 cycles under 60% of the maximum air pressure determined in the airtightness experiment. Across five tested samples, none exhibited leakage after 1,000 cycles, and no 3D-printed structures detached. Only the TPU film showed slight wrinkling due to minor plastic deformation.